



## Synthesis, characterisation, photochromic study of cadmium(II) halide complexes of 1-alkyl-2-methyl-4-(*p*-nitro-phenylazo)imidazole and DFT computation

Debashis Mallick<sup>a\*</sup>, Chandana Sen<sup>b</sup>, Mrinal Kanti Paira<sup>c</sup>, Basudeb Dutta<sup>d</sup>, Suman Kundu<sup>e</sup> and Chittaranjan Sinha<sup>f</sup>

<sup>a</sup>Department of Chemistry, Mrinalini Datta Mahavidyapith, Kolkata-700 051, India

E-mail: dmchemmdm51@gmail.com

<sup>b</sup>Department of Chemistry, Sripat Singh Collge, Murshidabad-742 123, West Bengal, India

<sup>c</sup>Department of Chemistry, Raja N. L. Khan College, Gope Palace, Paschim Medinipur-721 102, West Bengal, India

<sup>d</sup>Department of Chemistry, Aliah University, New Town, Kolkata 700 156, India

<sup>e</sup>Department of Chemistry, Ramakrishna Mission Residential College, Kolkata-700 103, India

<sup>f</sup>Department of Chemistry, Jadavpur University, Kolkata-700 032, India

Manuscript received online 16 June 2019, revised and accepted 10 July 2019

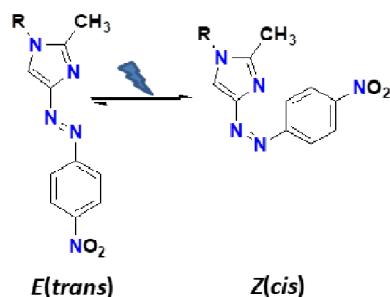
1-Alkyl-2-methyl-4-(*p*-nitro-phenylazo)imidazole complexes of Cd(II), Cd[ $\{p\text{-NO}_2\text{-aai(Me)R}\}_2\text{X}_2$  (**2-4**) [ $\{p\text{-NO}_2\text{-aai(Me)R} = 1\text{-alkyl-2-methyl-4-(}p\text{-nitro-phenylazo)imidazole}\}$ , {R = -CH<sub>3</sub> (**1a**), -C<sub>2</sub>H<sub>5</sub> (**1b**)} (X = Cl, Br, I)] have been synthesized and characterized by spectral (UV-Vis, IR, <sup>1</sup>H NMR) data and have been confirmed by single crystal X-ray diffraction study in the case *p*-NO<sub>2</sub>-aai(2-Me)1-C<sub>2</sub>H<sub>5</sub> (**1b**) and Cd[ $\{p\text{-NO}_2\text{-aai(2-Me)1-C}_2\text{H}_5\}_2\text{I}_2$ ] (**4b**). Both ligands and complexes undergo *E(trans)*-to-*Z(cis)* isomerization when irradiated with UV light. The reverse *Z(cis)*-to-*E(trans)* isomerization can be driven thermally in the dark. The rates and quantum yields ( $\phi_{E\rightarrow Z}$ ) of *E*-to-*Z* isomerisation are higher for free ligand, **1**, than their complexes, **2-4**. The activation energies ( $E_a$ ) and activation entropies ( $\Delta S$ ) of the *Z*-to-*E* isomerization are calculated by controlled temperature experiment (298–313 K). Effect of halides on the rate and quantum yields of photochromism is established and has been supported by DFT computation of optimized structures. Slow rate of photoisomerisation of coordinated ligands compare to the free ligands may be due to increased mass and rotor volume of the complexes. The rate of isomerization follows the sequence Cd[ $\{p\text{-NO}_2\text{-aai(2-Me)1-C}_2\text{H}_5\}_2\text{Cl}_2$ ] < Cd[ $\{p\text{-NO}_2\text{-aai(2-Me)1-C}_2\text{H}_5\}_2\text{Br}_2$ ] < Cd[ $\{p\text{-NO}_2\text{-aai(2-Me)1-C}_2\text{H}_5\}_2\text{I}_2$ ].

Keywords: Cd(II) complexes, ligand, X-ray structures, photoisomerisation, DFT computation.

### Introduction

Photochromism is the reversible transformation of a single molecule upon irradiation with light to another molecule where these two compounds have distinguishable absorption spectrum<sup>1</sup>. Upon continuous irradiation the organic photochromes may undergo photodegradation, photodissociation, photodamage while metallo-organic photochromes are very stable and more sensitive to optical properties. The photochromic property has been applied widely in diverse area, ranging from biomedical research to information technology<sup>1–7</sup>. The property may be varied by changing the nature of the ligands, substituents, different carbocyclic and heterocyclic rings, and also by using different metal ions. Besides,

the photochromism is influenced by the experimental condition such, solvent polarity, presence of innocent molecules in the solution, change in pH of the medium etc. Photochromes may undergo structural isomerization, *trans*-to-*cis*, upon irradiation with UV light, which can be reversed by either heating or irradiation with visible light<sup>8–10</sup>. Rod-shaped planar *trans* isomer is thermodynamically more stable compare to nonplanar bent *cis* isomer. Lifetime of *cis* isomer, in general, is less stable mainly influenced by the molecular structure as well as the surrounding environment<sup>11–15</sup>. The azoheterocycles have been extensively used as ligands in the syntheses of metal complexes<sup>15–19</sup> and in few cases the photochromic property (Scheme 1) of arylazoimidazole dyes have been explored<sup>19–28</sup>. The photochromism of 1-alkyl-2-



**Scheme 1.** Isomerization of 1-alkyl-2-methyl-4-(*p*-nitro-phenylazo)imidazole.

(arylo)imidazole<sup>20,21</sup> and their Cu(I)<sup>22</sup>, Zn(II)<sup>23</sup>, Cd(II)<sup>24</sup>, Hg(II)<sup>25</sup>, Pb(II)<sup>26</sup>, Bi(III)<sup>27</sup>, Pd(II)<sup>28</sup>, Ag(I)<sup>29</sup> complexes are reported in literature. The electron withdrawing group in the *para* position of phenyl ring may play important role in the structure as well as photochromic property of the compounds. In this work we use electron withdrawing group -NO<sub>2</sub> in the *para* position of phenyl ring to synthesize 1-alkyl-2-methyl-4-(*p*-nitro-phenylazo)imidazole and it is used to synthesize Cd(II) complexes. Both ligands and complexes are characterized by spectroscopic studies and by single crystal X-ray diffraction measurements. The photochromic activity of the ligands and complexes are explained by DFT computation of optimized structures.

## Experimental

### Materials:

All chemicals and solvents employed were commercially available and used as supplied without further purification. Cadmium halides were obtained from Loba Chemicals, Bombay, India. The ligands, 1-alkyl-2-methyl-4-(*p*-nitro-phenylazo)imidazoles were synthesized by reported procedure<sup>30</sup>.

### Physical measurements:

Elemental (C, H, N) analyses were carried by using a Perkin-Elmer 2400 CHN analyzer. Spectroscopic data both ligands and complexes were obtained using the following instruments: UV-Vis spectra from a Perkin-Elmer Lambda 25 spectrophotometer; IR spectra of both ligands and complexes were recorded with a Perkin-Elmer RX-1 FTIR spectrophotometer by using KBr pellets in the region 4000–400 cm<sup>-1</sup>. Photo excitation has been carried out using a Perkin-Elmer LS-55 spectrofluorimeter and <sup>1</sup>H NMR spectra were recorded from a Bruker (AC) 300 MHz FTNMR spectrometer.

## Preparation of compounds

*Synthesis of {1-ethyl-2-methyl-4-(*p*-nitro-phenylazo)imidazole}, *p*-NO<sub>2</sub>-aai(Me)C<sub>2</sub>H<sub>5</sub> (**1b**):*

2-Methyl-4-(*p*-nitro-phenylazo)imidazole was synthesized by the diazotization of *p*-nitro aniline in NaNO<sub>2</sub>/HCl at low temperature (0–5°C) and followed by coupling with 2-methylimidazole in aqueous sodium carbonate solution at pH 7. To dry THF solution (75 ml) of 2-methyl-4-(*p*-nitro-phenylazo)imidazole (2.5 g, 10.86 mmol), NaH (50% paraffin) (0.65 g) was added in small portion and stirred at cold condition on ice bath for 0.5 h. 1-Iodoethane (1.6 ml, 11.28 mmol) was added slowly under stirring condition for a period of 1 h and then warm for another 2 h on steam bath. The solution was evaporated to dryness, extracted with CH<sub>2</sub>Cl<sub>2</sub>, washed with NaOH solution (10%, 10 ml×3) and finally by distilled water (20 ml×3). The CH<sub>2</sub>Cl<sub>2</sub> extract was chromatographed over silica gel column prepared in ethyl acetate. The elution was performed by 1:10 ethyl acetate-acetonitrile mixture. On slow evaporation in air orange crystalline product was obtained. Compound (**1a**) was prepared under identical conditions. The yield varied in the range 60–68%.

Microanalytical data: Calcd. for C<sub>11</sub>H<sub>11</sub>N<sub>5</sub>O<sub>2</sub> (**1a**): C, 53.87; H, 4.52; N, 28.56. Found: C, 53.84; H, 4.55; N, 28.58%; FT-IR (ν, cm<sup>-1</sup>): 1625 (C=N), 1405 (N=N); UV-Vis (λ<sub>max</sub>/nm, ε × 10<sup>-3</sup> (M<sup>-1</sup> cm<sup>-1</sup>)): 326 (0.8), 367 (1.6), 454 (0.2); <sup>1</sup>H NMR (CDCl<sub>3</sub>) δ, ppm: 2.50 (3H, s, 2-CH<sub>3</sub>), 7.72 (1H, s, 5-H), 8.30 (2H, d, *J* 7.3 Hz, 7,11-H), 8.03 (2H, d, *J* 8.2 Hz, 8,10-H), 4.12 (3H, s, N-CH<sub>3</sub>). Microanalytical data: Calcd. for C<sub>12</sub>H<sub>13</sub>N<sub>5</sub>O<sub>2</sub> (**1b**): C, 55.59; H, 5.05; N, 27.01. Found: C, 55.72; H, 5.13; N, 26.94%; FT-IR (ν, cm<sup>-1</sup>): 1627 (C=N), 1403 (N=N); UV-Vis (λ<sub>max</sub>/nm, ε × 10<sup>-3</sup> (M<sup>-1</sup> cm<sup>-1</sup>)): 329 (0.7), 366 (1.4), 454 (0.3); <sup>1</sup>H NMR (CDCl<sub>3</sub>) δ, ppm: 2.52 (3H, s, 2-CH<sub>3</sub>), 7.71 (1H, s, 5-H), 8.31 (2H, d, *J* 7.7 Hz, 7,11-H), 8.01 (2H, d, *J* 8.2 Hz, 8,10-H), 4.01 (2H, q, *J* 6.7 Hz, N-CH<sub>2</sub>-), 1.52 (3H, t, *J* 5.8 Hz, N-CH<sub>2</sub>-CH<sub>3</sub>).

*Synthesis of [Cd{*p*-NO<sub>2</sub>-aai(Me)C<sub>2</sub>H<sub>5</sub>}<sub>2</sub>] (**4b**):*

To acetonitrile solution (10 ml) of CdI<sub>2</sub> (20.8 mg, 0.085 mmol), *p*-NO<sub>2</sub>-aai(Me)C<sub>2</sub>H<sub>5</sub> (**1b**) (45 mg, 0.173 mmol) in MeOH (20 ml) was added and stirred for 4 h. The solution was then filtered and slowly evaporated in air to isolate red colored crystalline compound. The yield was 47 mg (70 %). Other complexes were prepared under identical conditions and the yield varied in the range 65–75%.

Microanalytical data: Calcd. for  $C_{22}H_{22}N_{10}O_4CdCl_2$  (**2a**): C, 39.22; H, 3.29; N, 20.79. Found: C, 39.32; H, 3.31; N, 20.89%; FT-IR ( $\nu$ ,  $cm^{-1}$ ): 1595 (C=N), 1374 (N=N); UV-Vis ( $\lambda_{max}/nm$ ,  $\epsilon \times 10^{-3}$  ( $M^{-1} cm^{-1}$ )): 351 (3.5), 395 (5.3), 501 (0.4);  $^1H$  NMR (DMSO- $d_6$ )  $\delta$ , ppm: 2.38 (3H, s, 2-CH<sub>3</sub>), 8.18 (1H, s, 5-H), 8.33 (2H, d,  $J$  7.2 Hz, 7,11-H), 7.88 (2H, d,  $J$  8.3 Hz, 8,10-H), 4.06 (3H, s, N-CH<sub>3</sub>). Calcd. for  $C_{24}H_{26}N_{10}O_4CdCl_2$  (**2b**): C, 41.07; H, 3.76; N, 19.95. Found: C, 41.15; H, 3.70; N, 19.81%; FT-IR ( $\nu$ ,  $cm^{-1}$ ): 1593 (C=N), 1373 (N=N); UV-Vis ( $\lambda_{max}/nm$ ,  $\epsilon \times 10^{-3}$  ( $M^{-1} cm^{-1}$ )): 354 (3.7), 397 (5.2), 501 (0.3);  $^1H$  NMR (DMSO- $d_6$ )  $\delta$ , ppm: 2.40 (3H, s, 2-CH<sub>3</sub>), 8.19 (1H, s, 5-H), 8.34 (2H, d,  $J$  7.8 Hz, 7,11-H), 7.90 (2H, d,  $J$  8.3 Hz, 8,10-H), 4.03 (2H, q,  $J$  6.8 Hz, N-CH<sub>2</sub>-), 1.35 (3H, t,  $J$  5.7 Hz, N-CH<sub>2</sub>-\*CH<sub>3</sub>). Calcd. for  $C_{22}H_{22}N_{10}O_4CdBr_2$  (**3a**): C, 34.65; H, 2.91; N, 18.36. Found: C, 35.67; H, 2.85; N, 18.30%; FT-IR ( $\nu$ ,  $cm^{-1}$ ): 1594 (C=N), 1376 (N=N); UV-Vis ( $\lambda_{max}/nm$ ,  $\epsilon \times 10^{-3}$  ( $M^{-1} cm^{-1}$ )): 352 (3.6), 396 (5.3), 501 (0.2);  $^1H$  NMR (DMSO- $d_6$ )  $\delta$ , ppm: 2.40 (3H, s, 2-CH<sub>3</sub>), 8.19 (1H, s, 5-H), 8.34 (2H, d,  $J$  7.4 Hz, 7,11-H), 7.89 (2H, d,  $J$  8.4 Hz, 8,10-H), 4.05 (3H, s, N-CH<sub>3</sub>). Calcd. for  $C_{24}H_{26}N_{10}O_4CdBr_2$  (**3b**): C, 36.45; H, 3.31; N, 17.71. Found: C, 36.52; H, 3.39; N, 17.64%; FT-IR ( $\nu$ ,  $cm^{-1}$ ): 1596 (C=N), 1374 (N=N); UV-Vis ( $\lambda_{max}/nm$ ,  $\epsilon \times 10^{-3}$  ( $M^{-1} cm^{-1}$ )): 353 (3.8), 394 (5.4), 503 (0.4);  $^1H$  NMR (DMSO- $d_6$ )  $\delta$ , ppm: 2.41 (3H, s, 2-CH<sub>3</sub>), 8.20 (1H, s, 5-H), 8.35 (2H, d,  $J$  7.6 Hz, 7,11-H), 7.92 (2H, d,  $J$  8.3 Hz, 8,10-H), 4.02 (2H, q,  $J$  6.6 Hz, N-CH<sub>2</sub>-), 1.33 (3H, t,  $J$  5.9 Hz, N-CH<sub>2</sub>-\*CH<sub>3</sub>). Calcd. for  $C_{22}H_{22}N_{10}O_4CdI_2$  (**4a**): C, 30.84; H, 2.59; N, 16.35. Found: C, 30.81; H, 2.61; N, 16.38%; FT-IR ( $\nu$ ,  $cm^{-1}$ ): 1596 (C=N), 1377 (N=N); UV-Vis ( $\lambda_{max}/nm$ ,  $\epsilon \times 10^{-3}$  ( $M^{-1} cm^{-1}$ )): 351 (3.4), 396 (5.2), 502 (0.3);  $^1H$  NMR (DMSO- $d_6$ )  $\delta$ , ppm: 2.40 (3H, s, 2-CH<sub>3</sub>), 8.20 (1H, s, 5-H), 8.34 (2H, d,  $J$  7.3 Hz, 7,11-H), 7.92 (2H, d,  $J$  8.5 Hz, 8,10-H), 4.07 (3H, s, N-CH<sub>3</sub>). Calcd. for  $C_{24}H_{26}N_{10}O_4CdI_2$  (**4b**): C, 32.58; H, 2.96; N, 15.83. Found: C, 32.59; H, 2.93; N, 15.82%; FT-IR ( $\nu$ ,  $cm^{-1}$ ): 1597 (C=N), 1375 (N=N); UV-Vis ( $\lambda_{max}/nm$ ,  $\epsilon \times 10^{-3}$  ( $M^{-1} cm^{-1}$ )): 352 (3.6), 397 (5.3), 501 (0.4);  $^1H$  NMR (DMSO- $d_6$ )  $\delta$ , ppm: 2.42 (3H, s, 2-CH<sub>3</sub>), 8.21 (1H, s, 5-H), 8.35 (2H, d,  $J$  7.8 Hz, 7,11-H), 7.91 (2H, d,  $J$  8.2 Hz, 8,10-H), 4.03 (2H, q,  $J$  6.6 Hz, N-CH<sub>2</sub>-), 1.36 (3H, t,  $J$  5.7 Hz, N-CH<sub>2</sub>-\*CH<sub>3</sub>).

### X-Ray diffraction study

Dark red single crystals of **1b** (0.83×0.38×0.21 mm<sup>3</sup>) and **4b** (0.59×0.45×0.39 mm<sup>3</sup>) were collected from slow evapo-

ration of mother liquor. The suitable single crystals were mounted on a thin glass fiber with commercially available super glue. X-Ray single crystal structure data were collected on a Bruker Smart-CCD diffractometer equipped with a normal focus equipped with graphite monochromated Mo- $K_{\alpha}$  ( $\lambda = 0.71073 \text{ \AA}$ ) radiation. The crystallographic data are shown in Table 1. The unit cell parameters and crystal-orientation matrices were determined by least squares refinements of all reflections. The intensity data were corrected for Lorentz and polarisation effects and an empirical absorption correction were also employed using the SAINT program. Data were collected applying the condition  $I > 2\sigma(I)$ . All these structures were solved by direct methods and followed by successive Fourier and difference Fourier syntheses. Full matrix least squares refinements on  $F^2$  were carried out using SHELXL-97<sup>31</sup> with anisotropic displacement parameters for all non-hydrogen atoms. Hydrogen atoms were constrained to ride on the respective carbon or nitrogen atoms with isotropic displacement parameters equal to 1.2 times the equivalent isotropic displacement of their parent atom in all cases. Complex neutral atom scattering factors were used throughout for all cases. All calculations were carried out using SHELXS 97<sup>32</sup>, SHELXL 97<sup>31</sup>, PLATON 99<sup>33</sup>, ORTEP-3<sup>34</sup> program.

### Photometric measurements:

Absorption spectra were taken with a Perkin-Elmer Lambda 25 UV/Vis spectrophotometer in a 1×1 cm quartz optical cell maintained at 25°C with a Peltier thermostat. The light source of a Perkin-Elmer LS 55 spectrofluorimeter was used as an excitation light, with a slit width of 10 nm. An optical filter was used to cut off overtones when necessary. The absorption spectra of the *cis* isomers were obtained by extrapolation of the absorption spectra of a *cis*-rich mixture. Quantum yields ( $\phi$ ) were obtained by measuring initial *trans*-to-*cis* isomerization rates ( $\nu$ ) in a well-stirred solution within the above instrument using the equation,  $\nu = (\phi I_0/V)(1 - 10^{-Abs})$  where  $I_0$  is the photon flux at the front of the cell,  $V$  is the volume of the solution, and  $Abs$  is the initial absorbance at the irradiation wavelength. The value of  $I_0$  was obtained by using azobenzene ( $\phi = 0.11$ ) for  $\pi$ - $\pi^*$  excitation<sup>35</sup> under the same irradiation conditions.

The thermal *cis*-to-*trans* isomerisation rates were obtained by monitoring absorption changes intermittently for a *cis*-rich solution kept in the dark at constant temperatures ( $T$ ) in the range from 298–313 K. The activation energy ( $E_a$ ) and the

**Table 1.** Summarized crystallographic data for *p*-NO<sub>2</sub>aai(Me)C<sub>2</sub>H<sub>5</sub> (**1b**) and [Cd{*p*-NO<sub>2</sub>aai(Me)C<sub>2</sub>H<sub>5</sub>}<sub>2</sub>I<sub>2</sub>](**4b**)

Compd.	<i>p</i> -NO <sub>2</sub> aai(Me)C <sub>2</sub> H <sub>5</sub> ( <b>1b</b> )	[Cd{ <i>p</i> -NO <sub>2</sub> aai(Me)C <sub>2</sub> H <sub>5</sub> } <sub>2</sub> I <sub>2</sub> ]( <b>4b</b> )
Empirical formula	C <sub>12</sub> H <sub>13</sub> N <sub>5</sub> O <sub>2</sub>	C <sub>24</sub> H <sub>26</sub> N <sub>10</sub> O <sub>4</sub> I <sub>2</sub> Cd
Formula weight	259.27	884.75
Temperature (K)	294(2)	294(2)
Crystal system	Monoclinic	Monoclinic
Space group	<i>P</i> 21/ <i>n</i>	<i>C</i> 2/ <i>c</i>
Unit cell dimensions		
<i>a</i> (Å)	9.2317(7)	32.1640(19)
<i>b</i> (Å)	6.3912(4)	10.5003(6)
<i>c</i> (Å)	21.6944(16)	18.8305(10)
β (°)	101.107(3)	101.501(3)
<i>V</i> (Å) <sup>3</sup>	1256.03(15)	6232.0(6)
<i>Z</i>	4	8
μ(MoKα) (mm <sup>-1</sup> )	0.098	2.729
<i>D</i> <sub>calc</sub> (mg m <sup>-3</sup> )	1.371	1.886
λ (Å)	0.71073	0.71073
<i>hkl</i>	-12 < <i>h</i> < 12; -8 < <i>k</i> < 8; -28 < <i>l</i> < 28	-42 < <i>h</i> < 42; -14 < <i>k</i> < 13; -25 < <i>l</i> < 25
θ-range (°)	2.608–28.240	2.261–28.321
Total reflections	3072	7658
Refined parameters	175	375
R <sub>1</sub> <sup>a</sup> [ <i>I</i> > 2σ( <i>I</i> )]	0.0556	0.0437
WR <sub>2</sub> <sup>b</sup>	0.1349	0.0836
Goodness of fit	1.053	1.138
<sup>a</sup> R = Σ  F <sub>o</sub> -  F <sub>c</sub>   /Σ F <sub>o</sub>  . <sup>b</sup> wR <sub>2</sub> = [Σw(F <sub>o</sub> <sup>2</sup> - F <sub>c</sub> <sup>2</sup> ) <sup>2</sup> /Σw(F <sub>o</sub> <sup>2</sup> ) <sup>2</sup> ] <sup>1/2</sup> , w = 1/[σ <sup>2</sup> (F <sub>o</sub> ) <sup>2</sup> + (0.0778P) <sup>2</sup> + 9.4074P]; where P = ((F <sub>o</sub> <sup>2</sup> + 2F <sub>c</sub> <sup>2</sup> )/3).		

frequency factor (*A*) were obtained from the Arrhenius plot,  $\ln k = \ln A - E_a/RT$ , where *k* is the measured rate constant, *R* is the gas constant, and *T* is temperature. The values of activation free energy ( $\Delta G^*$ ) and activation entropy ( $\Delta S^*$ ) were obtained through the relationships,  $\Delta G^* = E_a - RT - T\Delta S^*$  and  $\Delta S^* = [\ln A - 1 - \ln(k_B T/h)]/R$  where *k<sub>B</sub>* and *h* are Boltzmann's and Planck's constants, respectively.

#### Computational methods:

All the calculations for [Cd{*p*-NO<sub>2</sub>-aai(Me)Et}<sub>2</sub>X<sub>2</sub>] (*X* = Cl (**2b**), Br (**3b**), I (**4b**)) were carried out with the density functional theory (DFT) method as implemented in GAUSSIAN 09 (G09) program package<sup>36</sup> and the calculations have been performed using the B3LYP exchange correlation functional<sup>37</sup> using Los Alamos effective core potential plus double zeta (LanL2DZ)<sup>38–40</sup> basis set along with the corresponding pseudo potential without any symmetry constrain for lead, bromide and iodide. The vibrational frequency calculation was also performed for complexes to ensure that the optimized geometries represent the local minima and there are only

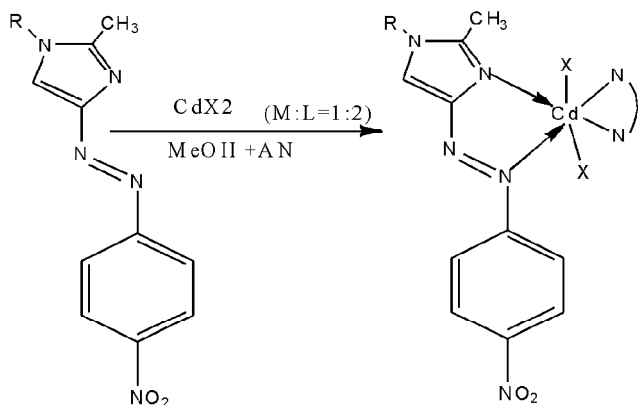
positive Eigen values. To assign the low lying electronic transitions in the experimental spectra, TD-DFT<sup>41</sup> calculations of the complexes were done. We computed the lowest 25 singlet-singlet transition and results of the TD-DFT calculations was qualitatively very similar. GaussSum<sup>42</sup> was used to calculate the fractional contributions of various groups to each molecular orbital.

## Results and discussion

#### Synthesis and formulation of the compounds:

2-Methyl-4-(*p*-nitro-arylazo)imidazole was synthesized by the diazotization of *p*-nitroaniline in NaNO<sub>2</sub>/HCl and followed by coupling with 2-methylimidazole in aqueous sodium carbonate solution (pH 7).

The alkylation was carried out by adding alkyl iodide in dry THF solution to the corresponding 2-methyl-4-(*p*-nitrophenylazo)imidazole in presence of NaH (Scheme 2). The ligand is unsymmetrical N,N'-bidentate chelator where N and N' refer to N(imidazolyl) and N(azo) donor centers, respec-



[Cd(*p*-NO<sub>2</sub>-aai(Me)CH<sub>3</sub>)<sub>2</sub>Cl<sub>2</sub>] (**2a**), [Cd(*p*-NO<sub>2</sub>-aai(Me)C<sub>2</sub>H<sub>5</sub>)<sub>2</sub>Cl<sub>2</sub>] (**2b**), [Cd(*p*-NO<sub>2</sub>-aai(Me)CH<sub>3</sub>)<sub>2</sub>Br<sub>2</sub>] (**3a**), [Cd(*p*-NO<sub>2</sub>-aai(Me)C<sub>2</sub>H<sub>5</sub>)<sub>2</sub>Br<sub>2</sub>] (**3b**), [Cd(*p*-NO<sub>2</sub>-aai(Me)CH<sub>3</sub>)<sub>2</sub>I<sub>2</sub>] (**4a**), [Cd(*p*-NO<sub>2</sub>-aai(Me)C<sub>2</sub>H<sub>5</sub>)<sub>2</sub>I<sub>2</sub>] (**4b**)

**Scheme 2.** Preparation of Cd(II) halide complexes.

tively. The reaction between *p*-NO<sub>2</sub>-aai(Me)R (R = -CH<sub>3</sub>-, C<sub>2</sub>H<sub>5</sub>) and CdX<sub>2</sub> in 2:1 mole ratio in MeOH and AN mixture has isolated compounds of chemical formula [Cd{(p-NO<sub>2</sub>-aai(Me)R)<sub>2</sub>X<sub>2</sub>}].

*Molecular structure of p-NO<sub>2</sub>-aai(Me)C<sub>2</sub>H<sub>5</sub> (1b):*

The crystal structure of (**1b**) is shown in Fig. 1 and selected bond parameters are listed in Table 2. Imidazole and *p*-nitro-phenyl groups are connected by -N=N- group and are

almost planar (deviation ~1.7°). Ethyl (-CH<sub>2</sub>CH<sub>3</sub>) group is about to perpendicular (~112.95°) on *p*-nitro-phenyl-azo-imidazole plane. The N=N bond length is 1.263(18) Å which is in support of reported data of other azoimidazole molecules<sup>43</sup>. The bonding strength between azo-N(4) and *p*-nitro-phenyl-[C(4)-N(4), 1.429(2) Å] is weaker than that of azo-N(3) and imidazolyl-C(3) [C(3)-N(3), 1.391(2) Å]. During the formation of supramolecular assembly there are some prominent hydrogen bonding interactions (Fig. 1b) ((intermolecular C(2)-H(2)---O(2) = 2.50 Å, (∠C(2)-H(2)---O(2) = 139°), (symmetry: -x, 1-y, 1-z)) and intermolecular C(11)-H(11B)---N(1) = 2.49 Å, (∠C(11)-H(11B)---N(1) = 163°), (symmetry: x, 1+y, z)) perform the pivotal role. There some parallel aromatic rings conform weak π...π interaction to form the self-assemble (Fig. 1c).

**Table 2.** Selected bond distances (Å) and angles (°) for *p*-NO<sub>2</sub>-aai(Me)C<sub>2</sub>H<sub>5</sub> (**1b**)

Bond lengths (Å)		Bond angles (°)	
C(3)-N(1)	1.375(2)	N(1)-C(3)-C(2)	110.59(14)
C(3)-C(2)	1.370(3)	N(1)-C(3)-N(3)	127.43(14)
C(2)-N(2)	1.358(2)	N(3)-C(3)-C(2)	121.97(15)
C(3)-N(3)	1.391(2)	C(3)-N(3)-N(4)	115.14(14)
N(3)-N(4)	1.263(18)	N(3)-N(4)-C(4)	113.23(13)
N(4)-C(4)	1.429(2)	N(4)-C(4)-C(5)	115.69(14)

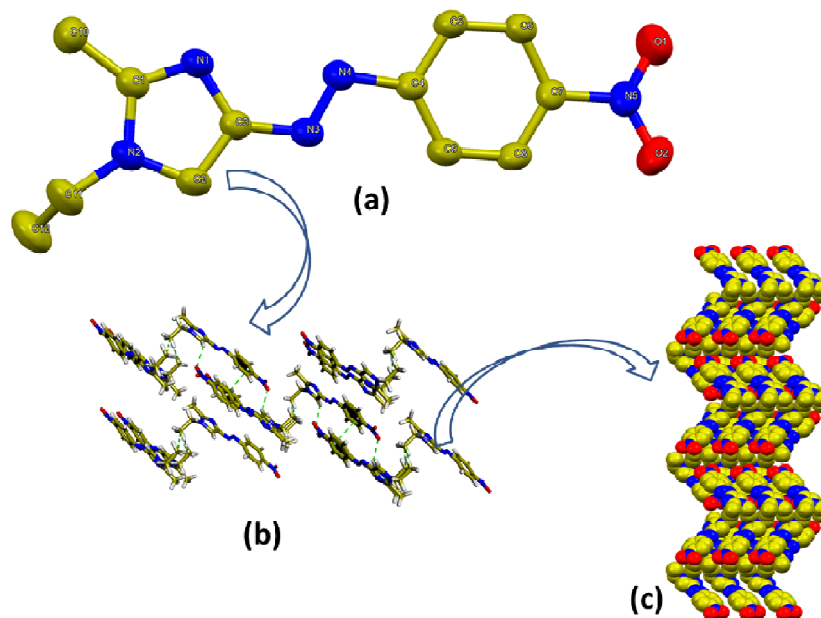


**Fig. 1.** The crystal structure of *p*-NO<sub>2</sub>-aai(Me)C<sub>2</sub>H<sub>5</sub> (**1b**): (a) Asymmetric molecular unit of ligand. (b) Different supra molecular interactions during the formation of assembly of ligand. (c) Space fill view along crystallographic axis **a** of supra molecular aggregate of ligand.

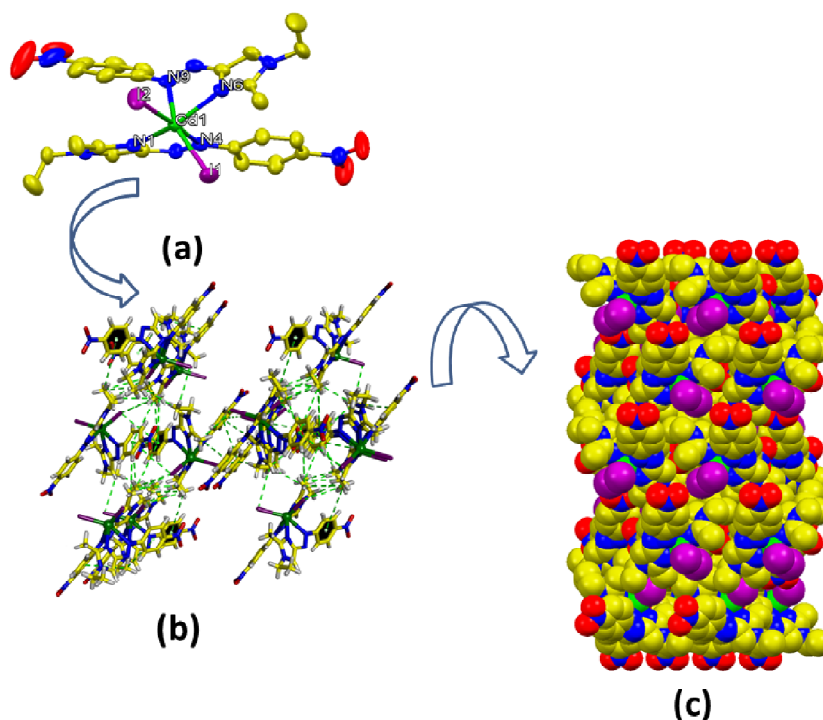


**Fig. 2.** The crystal structure of  $[\text{Cd}\{(p\text{-NO}_2\text{aai}(\text{Me})\text{C}_2\text{H}_5)_2\}_2\text{I}_2]$  (**4b**): (a) Asymmetric molecular unit of compound. (b) Different supra molecular interactions during the formation of assembly of compound. (c) Space fill view along crystallographic axis **a** of supra molecular aggregate of compound.

*Molecular structure of  $[\text{Cd}\{(p\text{-NO}_2\text{aai}(\text{Me})\text{C}_2\text{H}_5)_2\}_2\text{I}_2]$  (**4b**):*

The molecular structure of **4b** shows distorted octahedral orientation of the donor centres about Cd(II) (Fig. 2). Bond distances and angles are set out in Table 3. The metric parameters show distorted  $\text{CdN}_4\text{I}_2$  coordination sphere. The octahedral coordination is satisfied by chelating two  $p\text{-NO}_2\text{aai}(\text{Me})\text{C}_2\text{H}_5$  ligands and other two sites and charges are satisfied by two  $\text{I}^-$  ligands. The chelating N-Cd-N bond angles are  $\text{N}(1)\text{-Cd}(1)\text{-N}(4)$ ,  $63.77(10)^\circ$  and  $\text{N}(6)\text{-Cd}(1)\text{-N}(9)$ ,  $65.07(12)^\circ$  respectively. The Cd-N(azo) distances are the longest in the series and they are not equivalent:  $\text{Cd}(1)\text{-N}(4)$ ,  $2.597(3)$  and  $\text{Cd}(1)\text{-N}(8)$ ,  $2.805(3)$  Å. It is because the N(azo) requires considerably more room. The elongation of two Cd-N(azo) distance arises from lowering in overall symmetry of the geometry. However, the Cd-N(azo) distances are less than the sum of the van der Waals radii of Cd(II) ( $1.58$  Å) and N(azo) ( $1.55$  Å). This implies covalent interaction of N(azo) and Cd(II). In case of complex the hydrogen bonds (intramolecular  $\text{C}(11)\text{-H}(11\text{B})\cdots\text{O}(3) = 2.57$  Å, ( $\angle\text{C}(11)\text{-H}(11\text{B})\cdots\text{O}(3) = 143^\circ$ ), (symmetry:  $1/2-x, 5/2-y, 1-z$ ), intramolecular  $\text{C}(23)\text{-H}(23\text{A})\cdots\text{I}(1) = 3.00$  Å, ( $\angle\text{C}(23)\text{-H}(23\text{A})\cdots\text{I}(1) = 160^\circ$ ,

**Table 3.** Selected bond distances (Å) and angles ( $^\circ$ ) for  $[\text{Cd}\{(p\text{-NO}_2\text{aai}(\text{Me})\text{C}_2\text{H}_5)_2\}_2\text{I}_2]$  (**4b**)

Bond lengths (Å)		Bond Angles ( $^\circ$ )	
C(1)-N(1)	1.324(5)	N(2)-C(1)-N(1)	110.9(3)
C(3)-N(1)	1.380(5)	C(1)-N(1)-C(3)	105.2(3)
C(3)-C(2)	1.364(6)	C(3)-N(3)-N(4)	115.3(3)
C(3)-N(3)	1.383(3)	N(3)-N(4)-C(4)	112.8(3)
N(3)-N(4)	1.272(5)	N(4)-C(4)-C(5)	115.7(4)
N(4)-C(4)	1.427(5)	N(1)-Cd(1)-N(4)	63.77(10)
C(4)-C(5)	1.383(5)	N(6)-Cd(1)-N(9)	65.07(12)
N(1)-Cd(1)	2.338(3)	N(1)-Cd(1)-N(9)	79.09(11)
N(6)-Cd(1)	2.336(3)	N(4)-Cd(1)-I(1)	58.73(7)
N(4)-Cd(1)	2.805(3)	N(6)-Cd(1)-I(1)	101.17(9)
N(9)-Cd(1)	2.597(3)	N(4)-Cd(1)-I(2)	165.07(7)
I(1)-Cd(1)	2.7782(5)	N(6)-Cd(1)-I(2)	96.48(8)
I(2)-Cd(1)	2.8024(4)	N(9)-Cd(1)-I(1)	153.55(8)
		N(1)-Cd(1)-N(6)	139.63(11)
		I(2)-Cd(1)-I(1)	107.776(11)

\*Symmetry:  $-x, -y, -z$ ; \*\*Symmetry:  $1-x, 2-y, 1-z$ .

(symmetry:  $1-x, -1+y, 3/2-z$ ) and intermolecular  $\text{C}(24)\text{-H}(24\text{B})\cdots\text{O}(1) = 2.51$  Å, ( $\angle\text{C}(24)\text{-H}(24\text{B})\cdots\text{O}(1) = 156^\circ$ , (sym-

metry:  $x, 1-y, 1/2+z$ ) appear to form an assembly (Fig. 2b). Interestingly some intramolecular hydrogen bonding, weak C-H $\cdots\pi$  and  $\pi\cdots\pi$  interactions form the supramolecular architecture (Fig. 2c).

#### Spectral studies:

Two main infrared stretching frequencies are used as indicator of chelation of the ligand to Cd(II) :  $\nu_{N=N}$  and  $\nu_{C=N}$  in free ligand appear at  $1404\text{ cm}^{-1}$  and  $1626\text{ cm}^{-1}$  respectively while in the complexes these are observed at  $1375\text{ cm}^{-1}$  ( $\nu_{N=N}$ ) and  $1595\text{ cm}^{-1}$  ( $\nu_{C=N}$ ). The lowering of frequency in the complexes support the coordination of azo-N and imine-N to Cd(II). The absorption spectra were recorded in MeOH solution for the ligands and in DMF solution (because of sparing solubility of the complexes in MeOH) for the complexes, in the wavelength range 200–700 nm. The spectra of the ligands show absorption band at 360–370 nm with a molar absorption coefficient in the order of  $10^3\text{ M}^{-1}\text{ cm}^2$  and a weak band at 450–455 nm. The characteristics common to the complexes are a structured absorption band around 390–397 nm with a molar absorption coefficient on the order of  $10^3\text{ M}^{-1}\text{ cm}^2$  and a weak band at 500–505 nm ( $\epsilon \sim 10^3\text{ M}^{-1}\text{ cm}^2$ ). The transitions are shifted to longer wavelength by av. 25 nm in the case of complexes. This may due to the overlapping of MLCT transition from Cd(II)  $\rightarrow \pi^*$  (azoimine). The assignment is also supported by theoretical calculations, as described later. The  $^1\text{H}$  NMR spectra of ligands are recorded in  $\text{CDCl}_3$  and those of complexes are recorded in  $\text{DMSO-}d_6$  because of solubility problem in former solvent. Data reveal that the signals in the spectra, in general, are shifted downfield compared to the spectra of free ligand. The 7, 11-H are shifted to higher  $\delta$  by  $\sim 0.5$  ppm. The overall observation supports the existence of strong interaction between ligands and Cd(II) in the complexes. This conclusion is also supported by single crystal X-ray structure of one of the complexes (Fig. 2).

#### Photochromism:

Upon UV-light irradiation fixed at 3 min interval of  $\lambda_{\text{max}}$  to a MeOH solution of the ligands and DMF solution of complexes show the changes of absorption spectra those are corresponding to the structural change from *trans* (*E*-isomer) to *cis* (*Z*-isomer) (Figs. 3 and 4). The intense peak at  $\lambda_{\text{max}}$  decreases, which is accompanied by a slight increase at the tail portion of the spectrum until a stationary state is reached. Subsequent irradiation at the newly appeared longer wavelength peak reverses the course of the reaction and the

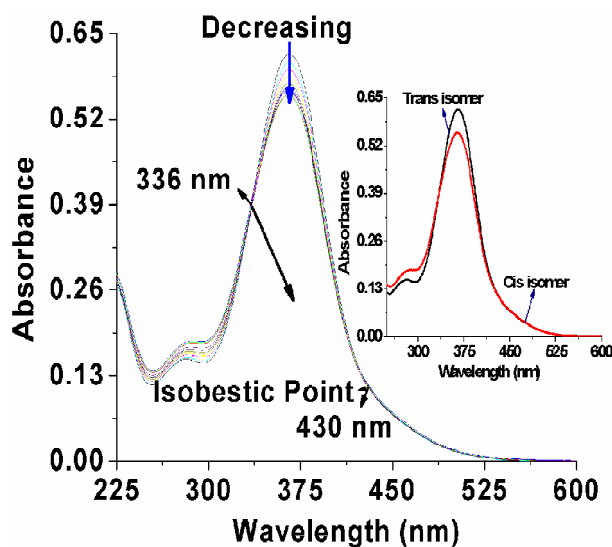


Fig. 3. Spectral changes of  $p\text{-NO}_2\text{aa}(\text{Me})\text{C}_2\text{H}_5$  (**1b**) in MeOH upon repeated irradiation at 364 nm at 3 min interval at  $25^\circ\text{C}$ ,

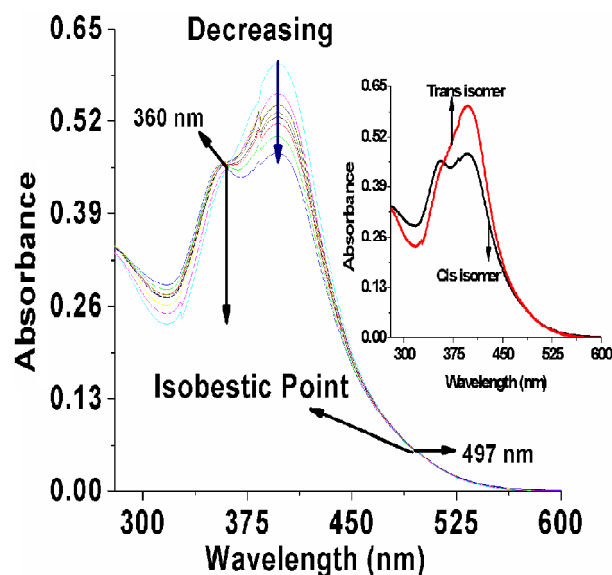


Fig. 4. Spectral changes of  $[\text{Cd}\{p\text{-NO}_2\text{-aa}(\text{Me})\text{C}_2\text{H}_5\}_2]_2$  (**4b**) in DMF upon repeated irradiation at 368 nm at 3 min interval at  $25^\circ\text{C}$ .

original spectrum is recovered up to a point, which is another photostationary state under irradiation at the longer wavelength peak. It is observed that upon irradiation with UV light *E*-to-*Z* change proceeds and the *Z* molar ratio is reached to  $\sim 70\%$  and  $65\%$  respectively for ligand and complexes. The ligands and the complexes show little sign of degradation upon repeated irradiation at least upto 14 cycles

**Table 4.** Results of photochromism, rate of conversion and quantum yields upon UV light irradiation

Compd.	$\lambda_{\pi,\pi^*}$ (nm)	Isobestic point (nm)	Rate of t $\rightarrow$ c conversion $\times 10^8$ (s $^{-1}$ )	$\phi_{t\rightarrow c}$ conversion
<b>1a</b>	367	337, 435	3.901	0.219 $\pm$ 0.002
<b>1b</b>	366	336, 430	3.316	0.196 $\pm$ 0.006
<b>2a</b>	395	361, 498	2.372	0.137 $\pm$ 0.002
<b>2b</b>	397	364, 497	2.194	0.124 $\pm$ 0.002
<b>3a</b>	396	362, 494	2.774	0.159 $\pm$ 0.003
<b>3b</b>	394	365, 491	2.371	0.137 $\pm$ 0.004
<b>4a</b>	396	363, 496	2.882	0.169 $\pm$ 0.002
<b>4b</b>	397	360, 497	2.422	0.141 $\pm$ 0.003

in each case. The quantum yields of the *E*-to-*Z* photoisomerization are determined using those of azobenzene<sup>25,35</sup> as a standard and the results are given in Table 4. The photoisomerisation rate and quantum yields of coordinated ligand are decreased compared to free ligand and in general, increase in mass of the molecule reduces the rate and quantum yield of isomerisation. Photo bleaching efficiency of halide<sup>44</sup> may snatch out energy from  $\pi$ - $\pi^*$  excited state. These may cause very fast deactivation other than photochromic route. Both rotor mass and volume are increased upon coordination of ligand to CdX<sub>2</sub>. These two factors have significant influence on the isomerisation rate and quantum yields.

The *Z*-to-*E* isomerisation of ligands (**1**) and its Cd(II) complexes (**2-4**) are followed by spectra measurements in MeOH and DMF, respectively at varied temperatures, 298–313 K. The Eyring plots in the range 298–313 K gave a linear graph from which the activation parameters  $\Delta S^\ddagger$  and  $\Delta H^\ddagger$  are calculated (Table 5, Fig. 5). In the complexes, the  $E_a$ s are severely reduced which means faster *Z*-to-*E* thermal isomerisation of the complex. The entropy of activation ( $\Delta S^\ddagger$ ) are high negative in the complexes than that of free ligand. This is also in support of increase in rotor volume of the complexes.

#### Electronic structure calculation and optical spectra:

The DFT and TD-DFT calculation have been performed using optimized structures of [Cd{*p*-NO<sub>2</sub>-aai(Me)C<sub>2</sub>H<sub>5</sub>}<sub>2</sub>X<sub>2</sub>] {X = Cl (**2b**), Br (**3b**), I (**4b**)}. In **2b** the HOMO and HOMO-1 are closely spaced ( $E_{\text{HOMO}}$ , -6.15 eV and  $E_{\text{HOMO-1}}$ , -6.22 eV) and composed of 93–96% contribution from bonded Cl (Fig. 6). The LUMO and LUMO+1 are also nearly degenerate  $\pi^*$  orbitals of 100% contribution of ligand *p*-NO<sub>2</sub>-aai(Me)C<sub>2</sub>H<sub>5</sub> ( $E_{\text{LUMO}}$ , -3.7 eV and  $E_{\text{LUMO+1}}$ , -3.68 eV). The HOMO-2 and other occupied levels differ both in energy and

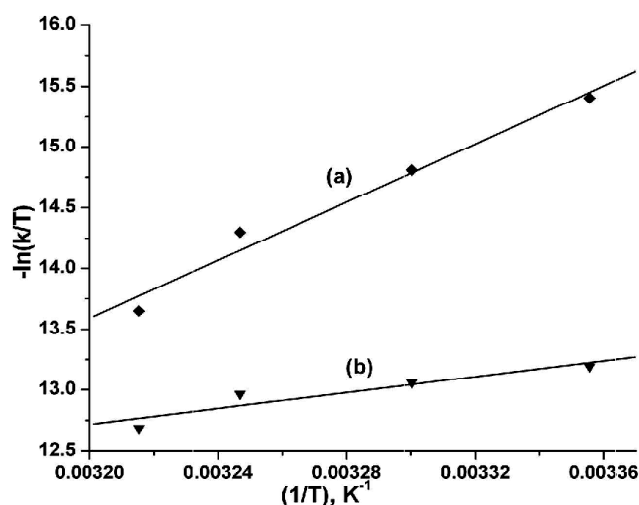


**Fig. 5.** The Eyring plots of rate constants of *Z*-to-*E* isomerisation of (a) *p*-NO<sub>2</sub>aai(Me)C<sub>2</sub>H<sub>5</sub> (**1b**) and (b) [Cd{*p*-NO<sub>2</sub>-aai(Me)C<sub>2</sub>H<sub>5</sub>}<sub>2</sub>]<sub>2</sub> (**4b**) at 298–313 K.

composition. LUMO+2 and higher unoccupied MOs also appear energetically at higher levels. The HOMO and HOMO-1 of **3b** contain 94–97% Br contribution. The characteristics of **4b** is also similar to **2b** and **3b** i.e. occupied MOs (HOMO, HOMO-1 etc.) have major contribution (95%) from I. The unoccupied MOs (LUMO, LUMO+1 etc.) are composed of mainly from *p*-NO<sub>2</sub>-aai(Me)C<sub>2</sub>H<sub>5</sub> ligand.

The transitions at longer wavelength are coming from X (Cl, Br or I)  $\rightarrow$   $\pi^*$ (azoimine) charge transfer (XLCT) transitions along with Cd-to-*p*-NO<sub>2</sub>-aai(Me)C<sub>2</sub>H<sub>5</sub> charge transfer transitions (mainly low intensities). They are calculated in between 625 and 270 nm. A strong  $\pi$ - $\pi^*$  transition (H-8/H-7 to L+1) is expected around 365–415 nm. The calculation shows that the XLCT (**2b**, **3b** and **4b**) transitions are of low intensities and the predictable bands appear in the range

**Table 5.** Rate and activation parameters for Z (c)  $\rightarrow$  E (t) thermal isomerisation

Compd.	Temp. (K)	Rate of thermal c $\rightarrow$ t conversion $\times 10^3$ (s $^{-1}$ )	$E_a$ (kJ mol $^{-1}$ )	$\Delta H^*$ (kJ mol $^{-1}$ )	$\Delta S^*$ (J mol $^{-1}$ K $^{-1}$ )	$\Delta G^{*c}$ (kJ mol $^{-1}$ )
<b>1a</b>	298	0.785	81.51	78.97	-58.58	96.86
	303	1.240				
	308	2.561				
	313	3.551				
<b>1b</b>	298	0.855	77.47	74.93	-71.44	96.75
	303	1.254				
	308	2.588				
	313	3.675				
<b>2a</b>	298	1.376	43.69	41.15	-180.98	96.44
	303	1.754				
	308	2.247				
	313	3.245				
<b>2b</b>	298	1.764	39.65	37.11	-191.96	95.75
	303	2.507				
	308	3.041				
	313	3.874				
<b>3a</b>	298	1.654	49.44	46.90	-160.78	96.02
	303	1.824				
	308	2.652				
	313	4.243				
<b>3b</b>	298	1.771	43.32	40.78	-179.71	95.68
	303	2.537				
	308	3.052				
	313	4.224				
<b>4a</b>	298	1.875	52.94	50.40	-147.61	95.50
	303	2.354				
	308	3.352				
	313	5.213				
<b>4b</b>	298	1.892	49.44	46.90	-158.82	95.43
	303	2.814				
	308	3.064				
	313	5.332				

between 500 and 340 nm while  $\pi - \pi^*$  transition is expected at 325–375 nm. The transitions of large oscillator strength ( $> 0.2$ ) are calculated at 414.97 (0.4252) (**2b**), 370.40 (0.4660) (**3b**) and 370.73 (0.3192) (**4b**) nm.

In photochromic process the UV light irradiation is mandatory to the molecule in solution for a fixed time which will enforce to isomerise more stable *trans*-isomer (E) to *cis*-isomer (Z). Irradiation in the UV region may be responsible to

$\pi \rightarrow \pi^*$  transition. The MLCT or XLCTs are of lower energetic transition which are capable to charge transfer to azoimidazole and may not sufficient to perform physical process like Cd-N(azo) cleavage or isomerisation. Conversely, the excited complex may perform charge transition in a secondary (MLCT or XLCT) process which is responsible for deactivation of excited species and reduces the rate of E  $\rightarrow$  Z change and quantum yields. This is observed, indeed (Table 7).

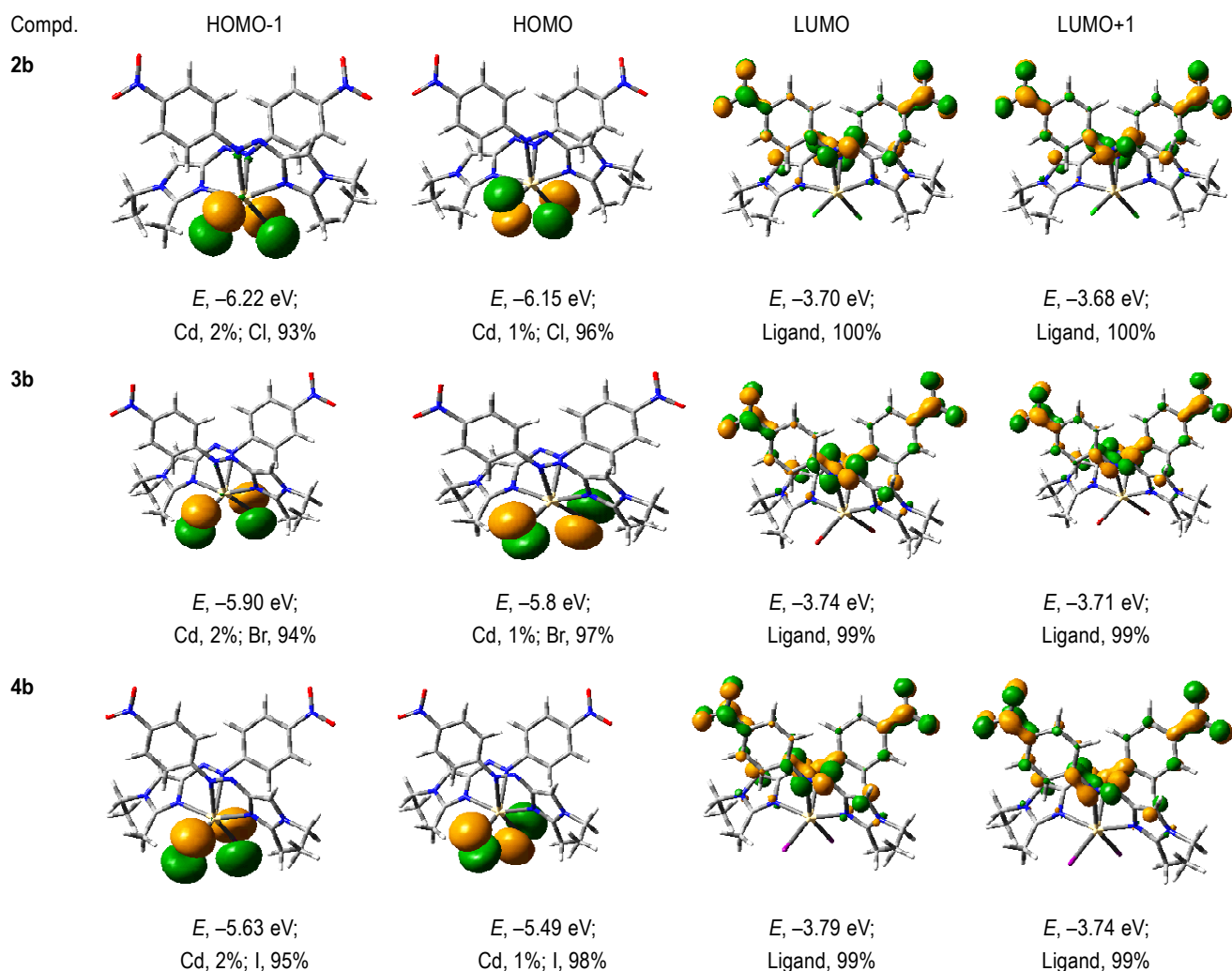


**Fig 6.** Surface plots of HOMO, HOMO-1, LUMO and LUMO+1 of  $[\text{Cd}\{p\text{-NO}_2\text{-aai}(\text{Me})\text{C}_2\text{H}_5\}_2\text{Cl}_2]$  (**2b**);  $[\text{Cd}\{p\text{-NO}_2\text{-aai}(\text{Me})\text{C}_2\text{H}_5\}_2\text{Br}_2]$  (**3b**) and  $[\text{Cd}\{p\text{-NO}_2\text{-aai}(\text{Me})\text{C}_2\text{H}_5\}_2\text{I}_2]$  (**4b**).

The correlation diagram (Fig. 7) shows energy sequence of MOs of the complexes. The energy ordering of MOs of  $[\text{Cd}\{p\text{-NO}_2\text{-aai}(\text{Me})\text{C}_2\text{H}_5\}_2\text{Cl}_2]$  and  $[\text{Cd}\{p\text{-NO}_2\text{-aai}(\text{Me})\text{C}_2\text{H}_5\}_2\text{Br}_2]$  are closely associated while energy of MOs of  $[\text{Cd}\{p\text{-NO}_2\text{-aai}(\text{Me})\text{C}_2\text{H}_5\}_2\text{I}_2]$  is higher than the respective MOs of previous complexes. Besides, the energy difference ( $\Delta E = E_{\text{LUMO}} - E_{\text{HOMO}}$ ) between HOMO and LUMO follows the ordering  $[\text{Cd}\{p\text{-NO}_2\text{-aai}(\text{Me})\text{C}_2\text{H}_5\}_2\text{I}_2]$  (1.7 eV) <  $[\text{Cd}\{p\text{-NO}_2\text{-aai}(\text{Me})\text{C}_2\text{H}_5\}_2\text{Br}_2]$  (2.06 eV) <  $[\text{Cd}\{p\text{-NO}_2\text{-aai}(\text{Me})\text{C}_2\text{H}_5\}_2\text{Cl}_2]$  (2.54 eV). The plots of  $\Delta E$  versus rates of isomerisation and quantum yields are linearly related (Fig. 8). This implies the direct correlation between photophysical process and activation energy barrier.

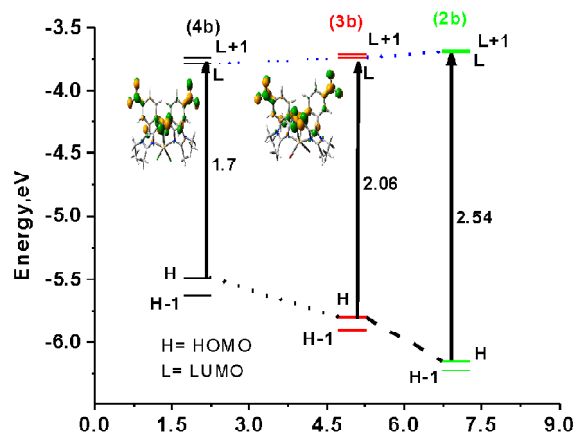


**Fig. 7.** Energy correlation between HOMO (H), HOMO-1 (H-1), LUMO (L) and LUMO+1 (L+1) of **2b**, **3b** and **4b**. Results obtained from DFT calculation of optimized geometries.

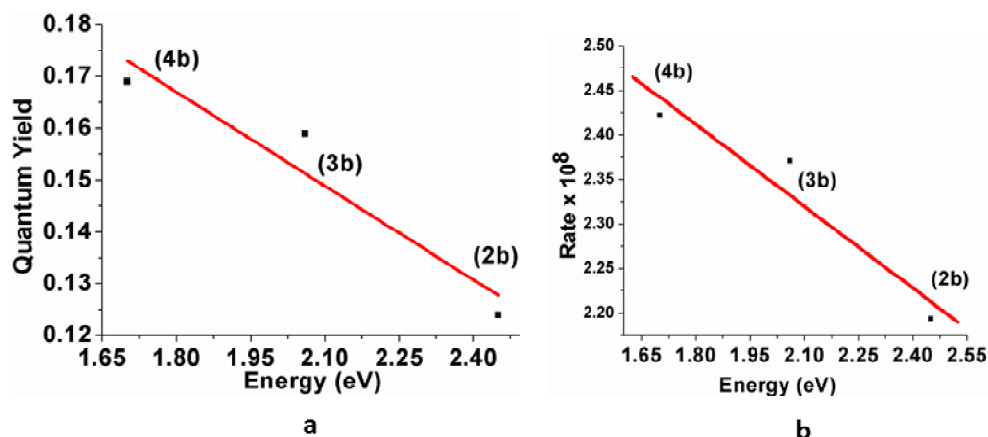


Fig. 8. Correlation between (a)  $\Delta E (= E_{LUMO} - E_{HOMO})$  vs quantum yields and (b)  $\Delta E (= E_{LUMO} - E_{HOMO})$  vs rates of photoisomerisation.

## Conclusions

In summary, *p*-NO<sub>2</sub>-aai(Me)R and [Cd{*p*-NO<sub>2</sub>-aai(Me)R}<sub>2</sub>X<sub>2</sub>] have been successfully synthesized, characterized and confirmed by single crystal X-ray diffraction study in case of *p*-NO<sub>2</sub>-aai(Me)C<sub>2</sub>H<sub>5</sub> and [Cd{*p*-NO<sub>2</sub>-aai(Me)C<sub>2</sub>H<sub>5</sub>}<sub>2</sub>I<sub>2</sub>]. Photochromism are examined by repetitive UV light irradiation in methanol solution for the ligand and the DMF solution is used for the complexes. The rate and quantum yields of *E*-to-*Z* isomerisation of the complexes is less than that of free ligand data. The rotor mass and volume may be the regulating agents for these data. The *E*-to-*Z* isomerisation is thermally driven process. The activation energy ( $E_a$ s) of isomerisation of the free ligand three times than that of the complex that implies the lowering of rate in the complex.

## Acknowledgements

DM thanks University Grants Commission for the Minor Research Project (F.PSW-158/13-14). One of the authors (CS) acknowledge for the financial support from the Council of Scientific and Industrial Research (CSIR, Sanction No. 01(2894)/17/EMR-II), New Delhi, India.

## Supporting information

Crystallographic data for the structures of *p*-NO<sub>2</sub>-aai(Me)C<sub>2</sub>H<sub>5</sub> (**1b**) and complex [Cd{*p*-NO<sub>2</sub>-aai(Me)C<sub>2</sub>H<sub>5</sub>}<sub>2</sub>I<sub>2</sub>] (**4b**) have been deposited with the Cambridge Crystallographic Data center, CCDC No. 1918932 (**1b**) and 1918933 (**4b**). Copies of this information may be obtained free of charge from the Director, CCDC, 12 Union Road, Cambridge

CB2 1EZ, UK (E-mail: deposit@ccdc.cam.ac.uk or www:htp://www.ccdc.cam.ac.uk).

## References

1. S. Kawata and Y. Kawata, *Chem. Rev.*, 2000, **100**, 1777.
2. S. R. Marder, in : D. W. Bruce and D. O'Hare (Eds.), "Metal Containing Materials for Nonlinear Optics in Inorganic Materials", 2nd ed., Wiley, Chichester, 1996, pp. 121-169.
3. O. R. Evans and W. Lin, *Acc. Chem. Res.*, 2002, **35**, 511.
4. P. Hbza and Z. Hablas, *Chem. Rev.*, 2000, **100**, 4253.
5. B. Cornils, W. A. Herrmann and R. Schlogl (Eds.), "Catalysis from A to Z: A Concise Encyclopedia", John Wiley & Sons, New York, 2000.
6. D. Demus, J. W. Goodby, G. W. Gray, H.-W. Spiess and V. Vill (Eds.), "Handbbook of Liquid Crystals", Wiley-VCH, Weinheim, 1998.
7. J. R. Farraro and J. M. Williams, "Introduction to Synthetic Electrical Conductors", Academic Press, New York, 1987.
8. H. Rau, "Photochromism: Molecules and Systems", ed. H. Durr and H. Bouas-Laurent, Elsevier, Amsterdam, 1990.
9. H. Zollinger, "Color Chemistry: Synthesis, Properties and Applications of Organic Dyes and Pigments", 2nd ed., VCH, Weinheim, 1991.
10. (a) K. Ichimura, *Chem. Rev.*, 2000, **100**, 1847; (b) O. Pieroni, A. Fissi, N. Angelini and F. Lenci, *Acc. Chem. Res.*, 2001, **34**, 9.
11. (a) P. D. Wildes and E. H. White, *J. Am. Chem. Soc.*, 1971, **93**, 2004; (b) G. Gabor and E. Fischer, *J. Phys. Chem.*, 1971, **75**, 581.
12. (a) C. S. Paik and H. Morawetz, *Macromolecules*, 1972, **5**, 171; (b) E. V. Brown and G. R. Granneman, *J. Am. Chem. Soc.*, 1975, **97**, 621.
13. (a) J. M. Nerbonne and R. G. Weiss, *J. Am. Chem. Soc.*, 1978, **100**, 5953; (b) H. J. Haitjema, Y. Y. Tan and G.

- Challa, *Macromolecules*, 1995, **28**, 2867; (c) C. Wang and R. G. Weiss, *Macromolecules*, 2003, **36**, 3833.
14. (a) Y. Norikane, K. Kitamoto and N. Tamaoki, *Org. Lett.*, 2002, **4**, 3907; (b) Y. Norikane, R. Katoh and N. Tamaoki, *Chem. Commun.*, 2008, **16**, 1898.
  15. U. Ray, D. Banerjee, G. Mostafa, Lu, T.-H. and C. Sinha, *New J. Chem.*, 2004, **28**, 1437.
  16. J. Dinda, S. Jasimuddin, G. Mostafa, C.-H. Hung and C. Sinha, *Polyhedron*, 2004, **23**, 793.
  17. J. Dinda, S. Senapati, T. Mondal, A. D. Jana, M. Chiang, T.-H. Lu and C. Sinha, *Polyhedron*, 2006, **25**, 1125.
  18. M. N. Ackermann, M. P. Robinson, I. A. Maher, E. B. LeBlanc and R. V. Raz, *J. Organomet. Chem.*, 2003, **682**, 248.
  19. T. Michinobu, R. Eto, H. Kumazawa, N. Fujii and K. Shigehara, *J. Macromol. Sci.*, 2011, **48A**, 625.
  20. J. Otsuki, K. Suwa, K. Narutaki, C. Sinha, I. Yoshikawa, and K. Araki, *J. Phys. Chem. A*, 2005, **109**, 8064.
  21. J. Otsuki, K. Suwa, K. K. Sarker and C. Sinha, *J. Phys. Chem. A*, 2007, **111**, 1403.
  22. K. K. Sarker, A. D. Jana, G. Mostafa, J.-S. Wu, T.-H. Lu and C. Sinha, *Inorg. Chim. Acta*, 2006, **359**, 4377.
  23. (a) P. Datta, D. Mallick, T. K. Mondal and C. Sinha, *Polyhedron*, 2014, **71**, 47; (b) C. Sen, B. Chowdhuri, C. Patra, D. Mallick and C. Sinha, *Spectrochimica Acta, Part A: Molecular and Biomolecular Spectroscopy*, 2015, **151**, 443.
  24. K. K. Sarker, D. Sardar, K. Suwa, J. Otsuki and C. Sinha, *Inorg. Chem.*, 2007, **46**, 8291.
  25. K. K. Sarker, B. G. Chand, K. Suwa, J. Cheng, T.-H. Lu, J. Otsuki and C. Sinha, *Inorg. Chem.*, 2007, **46**, 670.
  26. (a) D. Mallick, A. Nandi, K. K. Sarker, P. Datta, T. K. Mondal and C. Sinha, *Inorg. Chim. Acta*, 2012, **387**, 352; (b) D. Mallick, U. Panda, S. Jana, C. Sen, T. K. Mondal and C. Sinha, *Polyhedron*, 2013, **117**, 18; (c) D. Mallick, B. Chowdhury, C. Sen, K. K. Sarkar, S. Jana, S. Mondal and C. Sinha, *Indian J. Chem.*, 2018, **57A**, 418.
  27. D. Mallick, K. K. Sarker, R. Saha, T. K. Mondal and C. Sinha, *Polyhedron*, 2013, **54**, 147.
  28. P. Pratihari, T. K. Mondal, A. K. Patra and C. Sinha, *Inorg. Chem.*, 2009, **48**, 2760.
  29. (a) A. Nandi, C. Sen, S. Roy, D. Mallick, R. Sinha, T. K. Mondal and C. Sinha, *Polyhedron*, 2014, **79**, 186; (b) B. Chowdhury, K. Naskar, D. Mallick, K. K. Sarkar, C. Sen and C. Sinha, *Inorg. Chim. Acta*, 2018, **483**, 87.
  30. T. K. Misra, D. Das, C. Sinha, P. K. Ghosh and C. K. Pal, *Inorg. Chem.*, 1998, **37**, 1672.
  31. G. Zentai, L. Partain, R. Pavlyuchkova, C. Proano, G. Virshup, L. Melekshov, A. Zuck, B. N. Breen, O. Dagan, Vilensky, M. Schieber, H. Gilboa, P. Bennet, K. Shah, Y. Dimitriev, J. Thomas, M. Yaffe and D. Hunter, *Proc. SPIE MI-2003*, 2003, pp. 5030-5043.
  32. G. M. Sheldrick, SHELXS 97, Program for the Solution of Crystal Structure, University of Gottingen, Germany, 1997.
  33. G. M. Sheldrick, SHELXL 97, Program for the Solution of Crystal Structure, University of Gottingen, Germany 1997.
  34. A. L. Spek, PLATON, Molecular Geometry Program, University of Utrecht, The Netherlands, 1999.
  35. G. Zimmerman, L. Chow and U. Paik, *J. Am. Chem. Soc.*, 1958, **80**, 3528.
  36. Gaussian 03, Revision C.02, M. J. Frisch, G. W. Trucks, H. B. Schlegel, G. E. Scuseria, M. A. Robb, J. R. Cheeseman, J. A. Montgomery (Jr.), T. Vreven, K. N. Kudin, J. C. Burant, J. M. Millam, S. S. Iyengar, J. Tomas, V. Barone, B. Mennucci, M. Cossi, G. Scalmani, N. Rega, G. A. Petersson, H. Nakatsuji, M. Hada, M. Ehara, K. Toyota, R. Fukuda, J. Hasegawa, M. Ishida, T. Nakajima, Y. Honda, O. Kitao, H. Nakai, M. Klene, X. Li, J. E. Knox, H. P. Hratchian, J. B. Cross, V. Bakken, C. Adamo, J. Jaramillo, R. Gomperts, R. E. Stratmann, O. Yazyev, A. J. Austin, P. Cammi, C. Pomelli, J. W. Ochterski, P. Y. Ayala, K. Morokuma, G. A. Voth, P. Salvador, J. J. Dannenberg, V. G. Zakrzewski, S. Dapprich, A. D. Daniels, M. C. Strain, O. Farkas, D. K. Malick, A. D. Rabuck, K. Raghavachari, J. B. Foresman, J. V. Ortiz, Q. Cui, A. G. Baboul, S. Clifford, J. Cioslowski, B. B. Stefanov, G. Liu, A. Liashenko, P. Piskorz, I. Komaromi, R. L. Martin, D. J. Fox, T. Keith, M. A. Al-Laham, C. Y. Peng, A. Nanayakkara, M. Challacombe, P. M. W. Gill, B. Johnson, W. Chen, M. W. Wong, C. Gonzalez and J. A. Pople, Gaussian, Inc., Wallingford CT, 2004.
  37. B3LYP: A. D. Becke, *J. Chem. Phys.*, 1993, **98**, 5648.
  38. LanL2DZ: P. J. Hay and W. R. Wadt, *J. Chem. Phys.*, 1985, **82**, 270.
  39. W. R. Wadt and P. J. Hay, *J. Chem. Phys.*, 1985, **82**, 284.
  40. P. J. Hay and W. R. Wadt, *J. Chem. Phys.*, 1985, **82**, 299.
  41. EMSL, basis set library from <http://www.emsl.pnl.gov/forms/basisform.html>.
  42. N. M. O'Boyle and J. G. Vos, GaussSum 1.0; Dublin City, University, Dublin, Ireland, 2005.
  43. (a) J. Otsuki, K. Suwa, K. K. Sarker and C. Sinha, *J. Phys. Chem. A*, 2007, **111**, 1403; (b) A. Nandi, C. Sen, D. Mallick, R. K. Sinha and C. Sinha, *Advances in Materials Physics and Chemistry*, 2013, **3**, 133.
  44. A. T. Hutton and H. M. N. H. Irving, *J. Chem. Soc., Dalton Trans.*, 1982, 2299.